

The Effects of Random Surface and Pointing Deviations on GBT Performance

E. Wollack
NRAO, Charlottesville, VA
September 1, 1995

Introduction:

A telescope aperture is a coherent integrator which collects incident radiation for processing by a receiver. Deviations in the surface, pointing, and signal propagation introduce fluctuations in the phase across the aperture, thus, decreasing the integrator output. In the limit such processes do not adversely affect observations, ideal system performance is approached. We consider the GBT response with the projected surface figure and pointing noise. The telescope efficiency and angular response are briefly summarized.

An Idealized Beam Model:

The GBT main beam is well approximated by a Gaussian profile. We ignore the off-axis side-lobe response and frequency dependence of the illumination function in simplifying the following discussion. In this limit, the antenna gain is,

$$G(\theta) \simeq \frac{1}{2\pi\sigma_b^2} \exp\left(-\theta^2/2\sigma_b^2\right),$$

where the beam deviation is related to the beam full-width-half-maximum by $\sigma_b^2 \cong \theta_{\text{FWHM}}^2/8 \ln(2)$. By equating the antenna directivity, $D_o = \eta_a (\pi d/\lambda)^2$, with 4π over the total solid angle of the Gaussian beam, $\delta\Omega_o = 2\pi\sigma_b^2$, we estimate the beam constant for the primary,

$$\kappa \equiv \frac{d}{\lambda} \theta_{\text{FWHM}} \approx \frac{4}{\pi} \left(\frac{\ln(2)}{\eta_a} \right)^{1/2},$$

where d is the main reflector diameter, λ is observing wavelength, and η_a is the product of the spill, phase, and illumination efficiencies of the ideal aperture surface. We estimate for the GBT, $\kappa \approx 1.24$ radians (0.26×10^6 arc-seconds). We adopt this value for computing the beam size for an error-free system.

Finite Surface Errors:

Consider the effect of small random deviations in a reflector surface with a uniform illumination. Upon averaging the path length deviations, δr , over the surface, one finds that the directivity is reduced by a factor of

$$\langle \exp(ik\delta r) \rangle_r^2 = \exp(-k^2\sigma_r^2) \simeq \exp(-(4\pi\epsilon/\lambda)^2), \quad (1)$$

where $k = 2\pi/\lambda$ and ϵ is the rms of the surface measured with respect to the normal [1]. The factor of two increase in the rms, $2\epsilon \cong \sigma_r$, originates from the phase error incurred upon reflection from the surface. The surface efficiency is also a weak function of the illumination function and surface curvature. In practical applications, the surface efficiency is well approximated by

$$\eta(\epsilon) \simeq \frac{K + 1}{K + \exp(4\pi\epsilon/\lambda)^2},$$

where $K \cong x/\ln(1+x) - 1$ with $x \equiv (d/4f)^2$ [2]. In the large f limit, $K \rightarrow x/2 - x^2/12 + \dots \ll 1$, the Ruze theory is recovered. In the top panel of Figure 1, the surface efficiency is presented for the three phases of the GBT main surface alignment [3]¹. See Table 1 for the surface rms specification for each phase of construction.

Finite Pointing Errors:

The effect of noise in the telescope pointing can be examined by considering the spatial filtering properties of the telescope [6, 7]. The window function's high spatial frequency response is determined by the finite beam size. The low frequency response is a function of the observing strategy used to calibrate and control baseline drifts. Deviations in the source-to-beam-angle, originating from tracking errors, wind, or atmospheric scintillation, reduce the average receiver output for objects which are small compared to the beam. The amplitude of static structures large compared to the beam and pointing error scales, are essentially unaffected by the averaging process (the temporal-spatial average is a low-pass filter).

For pointing errors where the aperture phase coherence is preserved, the beam size increases due image blur. Examples include rigidly dithering the entire telescope and small feed-reflector differential motions. The instantaneous beam size is determined by the aperture; however, the average beam size is increased due to the motion during a sample period. If we assume that the telescope uses open-loop tracking to point at a source with a known position and the beam solid angle is stable in time, the reduction in directivity relative to a system with error-free tracking is

$$\eta(\sigma_\theta) = \left\langle \frac{\delta\Omega_o}{\delta\Omega(\sigma_\theta)} \right\rangle_t \simeq \delta\Omega_o \int_\Omega G(\theta_x, \theta_y) \left[\frac{e^{-\theta_x^2/2\sigma_\theta^2(AZ) - \theta_y^2/2\sigma_\theta^2(EL)}}{2\pi\sigma_\theta(AZ)\sigma_\theta(EL)} \right] d\theta_x d\theta_y,$$

¹For an off-axis parabolic reflector, the effective focal length is $f = 2f_o/(1 + \cos(\theta_o))$, where f_o is the focal length of the parent parabola and θ_o is the feed offset angle. For GBT main reflector the dish has $d = 100$ m, $f_o = 60$ m and $\theta_o = 45.5^\circ$ [4]. The aperture efficiency for the differing receiver bands ranges from $0.71 < \eta_a < 0.75$ [5]. In these calculations, an aperture efficiency of $\eta_a = 0.73$ is assumed.

where the term in brackets is the probability density, $P(\theta)$, for the system to experience an azimuthal or elevation pointing error ². Computing the expectation, value we find

$$\eta(\sigma_\theta) = \left(1 + \sigma_\theta^2(AZ)/\sigma_b^2\right)^{-1/2} \left(1 + \sigma_\theta^2(EL)/\sigma_b^2\right)^{-1/2}, \quad (2)$$

where for the GBT the rms azimuthal and elevation pointing errors are unequal, $\sigma_\theta(AZ) \sim 50 \sigma_\theta(EL)$. In the limit, $\sigma_\theta \gg \sigma_b$, the effective beam size approaches σ_θ . Beam motions which are an appreciable fraction of the source size result in poor integration efficiency. In the bottom panel of Figure 1, $\eta(\sigma_\theta)$ is given for selected rms pointing errors. See Table 2 for the anticipated GBT rms pointing performance under various wind velocities (for wind speed statistics at the site, see [11]). A summary of the effects of surface and pointing errors on the effective azimuthal beam size is presented in Figure 2.

Reductions in directivity due to time varying structural modes which distort the aperture phase can be expressed as a temporal average analogous to Equation 1. In this limit, the beam profile is not constant in time. However, we note that the focus tracking and panel actuators can be updated to remove correlated errors larger than the panel scale and that their noise is small. The remaining errors will be slowly varying functions of time which allow beam calibration on time scales rapid compared to an appreciable change in the antenna gain. To the extent these ‘quasi-static’ conditions are met, the resultant pointing errors modify the pointing coefficients with negligible variance.

²The transfer function of the telescope structure and the wind/slewing excitation spectrum admittedly result in a more complex response than the frequency independent power spectrum of pointing errors implicitly assumed. Such ‘systematic’ pointing errors are better represented as randomly driven telescope motions. Their effects may be estimated by using the path integral over beam trajectories,

$$P(\theta) \propto e^{-1/2 \int \int \theta(t) A^{-1}(t-t') \theta(t') dt dt'} \propto e^{-1/2 \int |\theta(\omega)|^2 A^{-1}(\omega) d\omega/2\pi},$$

for the probability density, where the kernel, $A^{-1}(t-t')$, is the inverse of the correlation function. If we assume for simplicity that the arm motion can be described as a damped harmonic oscillator, the scattering loss can be parameterized as a function of $\omega_o \tau_s (1 - 2\tau_m/\tau_s)/2Q$ and the pointing noise. Taking $\omega_o \simeq 2\pi(0.8\text{Hz})$ as the cross-elevation mode resonant frequency, $Q \sim 100$ as the ratio of stored-to-lost energy in the arm, $\tau_s = \tau_o f_o/f \sim 3 \times 10^3 [\text{sec GHz}]/f$ as the phase calibration time scale (Communication: T. Beasley, VLA), and $2\tau_m/\tau_s < 1$ for the ratio of the total slew time to the calibration period; a qualitative change in pointing performance occurs near $f_c \sim 20 \text{ GHz}$. For observing frequencies small compared to f_c , the arm motion has time to settle before the data on the source is acquired and reasonable integration efficiency can be achieved. For frequencies approaching and greater than f_c , the excitations do not have time to appreciably damp before the next motion required for phase calibration. Thus, the structure’s dynamics dictate the maximum deviation amplitude allowed in repointing the telescope for precision high frequency observations (~ 2 arc-seconds for Q-band). This noise can be minimized in the servo design by limiting the excitation from a commanded move. Further amplitude reductions can potentially be achieved by compensating for residual arm motions with active damping [8].

Conclusion:

The telescope efficiency is reduced by both the surface and pointing errors discussed; however, one fundamental difference should be noted. The reduction in gain due to the surface quality essentially increases the diffuse scattering to large angular scales (*ie.* increases the spill-over contribution to the system temperature and therefore the susceptibility to baseline drift). The gain reductions due to coherent motions of the telescope beam contribute to the noise as a gain variation term dependent upon the source spatial frequency distribution and temporal sampling. Ultimately, this increases the likelihood of systematic artifacts in an image due to aliased high spatial frequency noise.

[1] Ruze, J., 'The Effect of Aperture Errors on the Antenna Radiation Pattern,' *Proc. IEEE*, 1966, vol. 54, no. 4, pp. 633–642.

[2] Rahmat-Samii, Y., 'An Efficient Computational Method for Characterizing the Effects of Random Surface Errors on the Average Power Pattern of Reflectors,' *IEEE Trans. Ant. Propag.*, 1983, vol. AP-31, no. 1, Jan., pp. 92–98.

[3] Norrad, R.D., 'GBT Surface Accuracy,' 1995, GBT Memo #119.

[4] King, L., GBT Drawing, no. C35102M01, Rev. B, 1993.

[5] Srikanth, S., 'Gain Reduction Due to Gravity-Induced Deflections of the GBT Tipping Structure (Model 95, Version B),' 1994, GBT Memo #115 (also see GBT Memo #121).

[6] Safak, M., 'Limitations on Reflector Antenna Gain by Random Surface errors, Pointing Errors, and the Angle-of-Arrival Jitter,' *IEEE Trans. Ant. Propag.*, 1990, vol. AP-38, no. 1, Jan., pp. 117–121.

[7] Knepp, D., 'Aperture Antenna Effects After Propagation Through Strongly Disturbed Random Media,' *IEEE Trans. Ant. Propag.*, 1985, vol. 33, no. 10, Oct., pp. 1074–1084.

[8] Payne, J.M., and Emerson, D.T., 'Active Damping for the GBT Arm,' 1995, GBT Memo #133.

[9] Gawronski, W and Parvin, B., 'Modeling and Analysis of the Green Bank Telescope Control System,' 1995, GBT Memo #129, pp. 8–11, 14.

[10] Gawronski, W. and Parvin, B., 'Low Rate Simulations of the GBT Antenna with Dry Friction and Sticking, Report 2B,' 1995, GBT Memo #134, pp. 2-5.

[11] McKinnon, M.M., 'The Statistics of Wind Speed Near the GBT,' GBT Memo # 126.

TABLE 1
SURFACE RMS ERROR

Phase	ϵ [mm]	f_ϵ [GHz]
I	1.2	20
I [†]	0.48	50
II	0.35	70
III	0.23	100

The minimum beam size occurs at $f_\epsilon \cong c/4\pi\epsilon$. At this frequency the antenna gain is reduced by a factor of e (-4.34 dB) relative to an error-free aperture due to surface imperfections. The entry with a ‘†’ is the Phase I surface specification at the rigging angle.

TABLE 2
POINTING RMS ERROR

σ_θ [arc-seconds]	v_{wind} [m/sec]	f_{σ_θ} [GHz]
1	1.7	320
2	2.4	160
4	3.5	82
8	4.9	41
16	6.9	20
32	9.8	10
64	14	5

A $\sigma_\theta(v_{\text{wind}}) \sim 3''(v_{\text{wind}}/[3 \text{ m/sec}])^2$ scaling is assumed in estimating the wind-induced pointing errors [9]. The GBT design specification for a 7 m/sec wind (steady state and gusting) is 14 arc-seconds rms. The small σ_θ limit of the pointing performance is determined by switching induced vibrations and stiction-friction (The stiction-friction limit is a function of the azimuth drive rate. For rates greater than ~ 1 mdeg/sec (4.4 mdeg/sec is the sidereal rate), the $\sim 3''$ transients produced in initiating motion, decay in time. At 0.3 mdeg/sec, the pointing noise is $\sim 3''$ rms and sustained [10]). In the estimate it is assumed that the pointing errors are dominated by the excitation of the cross-elevation mode, $\sigma_\theta^2 \approx \sigma_\theta^2(\text{AZ}) \gg \sigma_\theta^2(\text{EL})$. Thus, the antenna gain is reduced by a factor of $\sqrt{2}$ (-1.5 dB) relative to an ideal antenna due to pointing jitter at $f_{\sigma_\theta} \cong \sqrt{2} c/\pi \sqrt{\eta_a} d \sigma_\theta$.

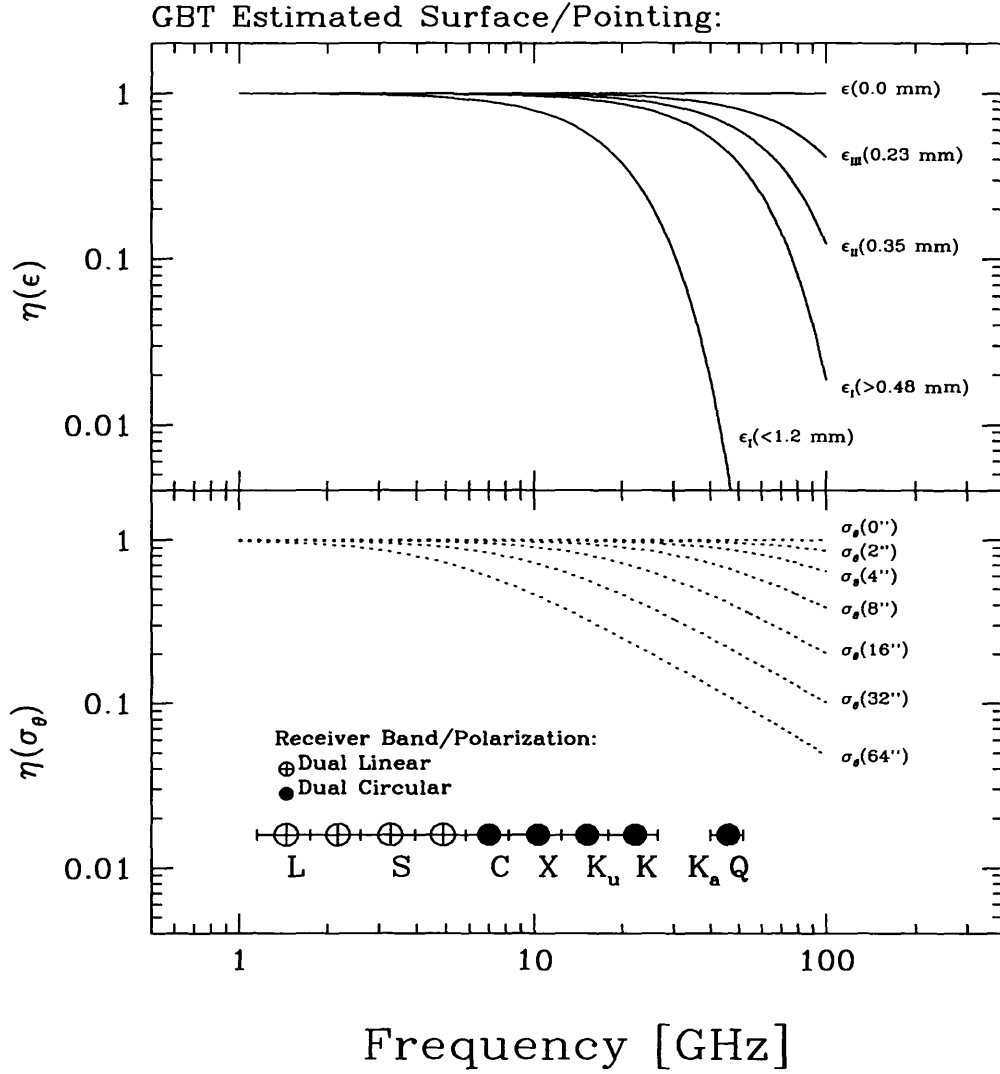


Figure 1. GBT Estimated Surface and Pointing Efficiency. The solid curves are the efficiencies for the indicated surface rms, ϵ in millimeters. The dashed curves are the efficiencies for the indicated rms pointing tolerance, σ_θ in arc-seconds. The beam sensitivity is $\Gamma = \eta_{\text{eff}} A_o / 2k_b \simeq [2.1 \text{ K/Jy}] \eta(\epsilon) \eta(\sigma_\theta)$, where $A_o = \pi d^2/4$ is the aperture area and $\eta_{\text{eff}}(f) = \eta_a \eta(\epsilon) \eta(\sigma_\theta)$ is the effective telescope efficiency.

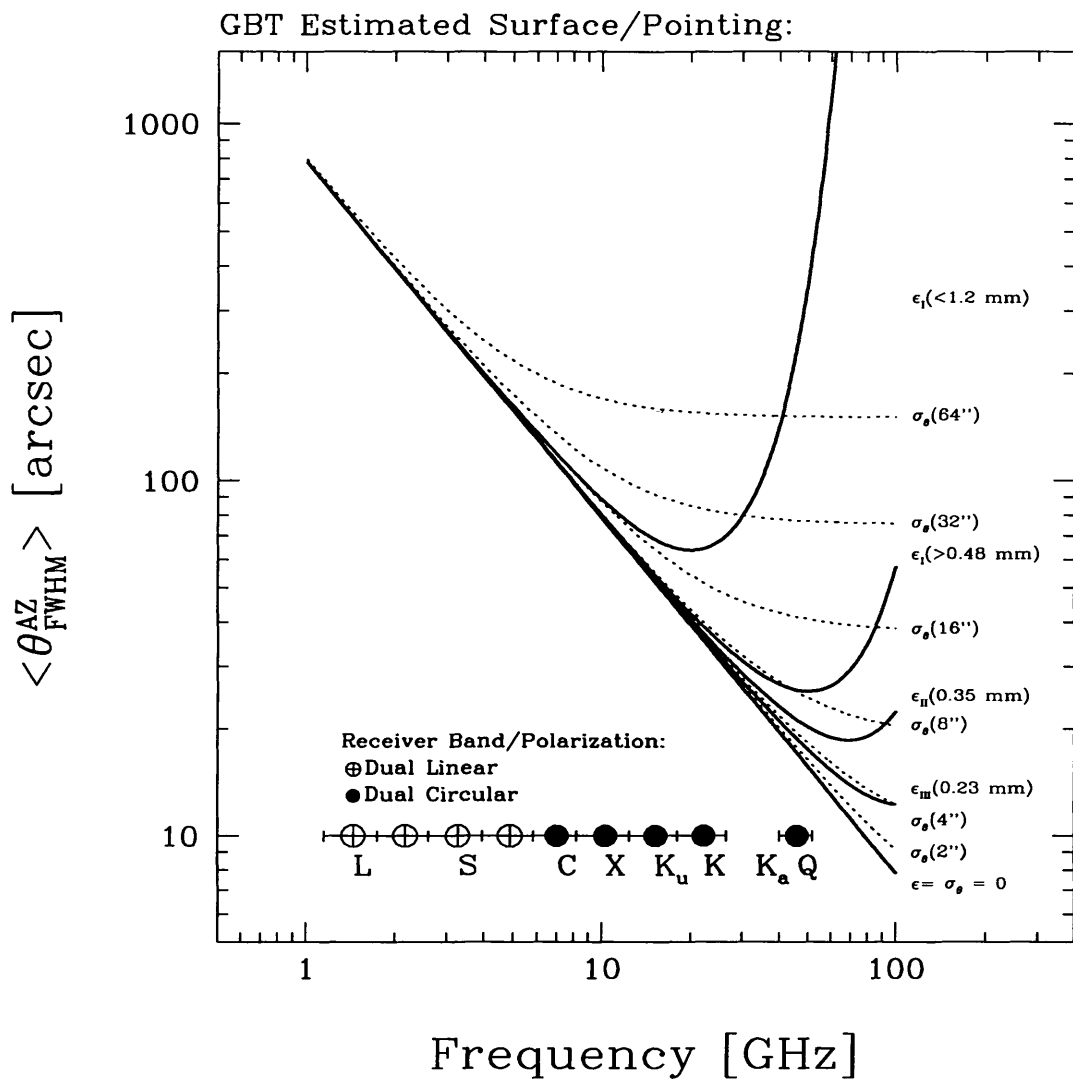


Figure 2. GBT Estimated Beam Broadening due to Surface and Pointing Deviations. The solid curves are for the indicated surface rms, ϵ in millimeters, with zero pointing error. The dashed curves are for the indicated rms pointing tolerance, σ_θ in arc-seconds, and an ideal surface.